DYNAMICAL MAP FOR COMBINED FUNCTION MAGNETS WITH SOLENOID, DIPOLE, AND QUADRUPOLE FIELDS*

A. Wolski[†] and M. Venturini[‡]

Lawrence Berkeley National Laboratory, Berkeley, CA 94720 USA.

Abstract

The interaction regions of colliders invariably include strong solenoid fields. Where quadrupoles and dipoles are embedded in the solenoid, the beam dynamics in the combined fields can be complicated to model using the traditional approach of interleaving slices of the different fields. The complexity increases if the design trajectory is offset from the magnetic axis; this is the case, for example, in PEP-II. In this paper, we present maps for combined solenoid, dipole and quadrupole fields that provide a much simpler alternative to the traditional approach, and show that the deviation of the design trajectory from the magnetic axis can be handle in a straightforward manner. We illustrate the techniques presented by reference to the PEP-II interaction region.

INTRODUCTION

Most lattice design codes (MAD [1] is an example) do not allow for a combined function magnetic element with superposed solenoidal, dipole, and quadrupole field components. As a consequence, modelling the interaction regions of colliders where several dipole and quadrupole magnets are often contained within the aperture of large solenoids requires a tedious procedure of interleaving slices of each field separately. While the resulting particle dynamics can still be accurately described, the required number of slices may be very large, making the effort time consuming, prone to implementation errors, and possibly impractical if the goal is to fit measured beam data. It is therefore desirable to extend these codes to include the transfer map for the combined function element.

Under the assumption that all the field components of interest (solenoid, quadrupole, and dipole) are invariant along a preferred direction (say, the solenoid axis) the calculation of the linear transfer map is easily done by solving an inhomogeneous linear system of first-order differential equations with constant coefficients. In this paper we outline the calculation, reporting some of the relevant formulas, and show a comparison with the slice model implemented in the MAD deck currently used for the PEP-II interaction regions.

TRANSFER MAP

The relevant Hamiltonian for the calculation of the desired linear transfer map including dispersive effects is

$$
\begin{aligned}
H \;=\; & \frac{1}{2}\left(1+\frac{P_\tau}{\beta_0}\right)\left[\left(p_x+\frac{1}{2}k_s y\right)^2\right.\\
& \left.+\;\left(p_y-\frac{1}{2}k_s x\right)^2\right]+k_0 x+\frac{k_1(x^2-y^2)}{2}.
\end{aligned}
$$

where, following the MAD notation $k_s = B_0/B\rho$, $k_0 = B_y/B\rho$, $k_1 = (\partial B_y/\partial x)/B\rho$, are the solenoid, dipole, quadrupole coefficients respectively, with $B\rho$ being the rigidity. The solenoid field B_0 points to the z−direction; the dipole field in the vertical y−direction. P_τ equals $-\Delta E/(p_0 c)$ where ΔE is the energy deviation from design value; p_0 is the design momentum.

As the energy deviation P_τ is a constant of the motion this dynamical system is effectively only four dimensional. The evolution of the time of flight can be determined later after solving the canonical equations for the transverse variables. Having denoted $\zeta = (x, p_x, y, p_y)$ the resulting linear canonical equations can be written in terms of a matrix A and vector $b = (0, -k_0, 0, 0)$ as $\frac{d\zeta}{dz} = A\zeta + b$ The solution with initial conditions $\zeta(z = 0) = \zeta_0$, $\zeta(z) = M(z)\zeta_0 + r(z)$ with $r = \int_0^z dz' M^{-1}(z')b$ requires determining $M(z) = \exp(Az)$, which can be done by diagonalizing A. The expressions for M and r can be written in relatively simple form upon a suitable grouping of the variables.

Having introduced the definitions $d = 1 + P_\tau/\beta_0, g = k_s/2$ and $S = \sqrt{4\,d^2\,g^4 + k_1{}^2}$ the eigenvalues for the matrix A, $\pm\lambda_1$ and $\pm i\lambda_2$ read $\lambda_1 = \sqrt{d}\sqrt{S - 2dg^2}, \lambda_2 = \sqrt{d}\sqrt{S + 2dg^2}$. With the additional definitions $P = S + k_1, P_+ = P + 2\,d\,g^2, P_- = P - 2\,d\,g^2, Q = S - k_1, Q_+ = Q + 2\,d\,g^2, Q_- = Q - 2\,d\,g^2$ we find the independent entries of the matrix M to be

$$
M_{11} = \frac{P\,\cos(z\,\lambda_2)}{2\,S} + \frac{Q\,\cosh(z\,\lambda_1)}{2\,S},
$$

$$
M_{12} = -\frac{\sinh(z\,\lambda_1)\,Q_+\,\lambda_1}{2k_1\,S} + \frac{\sin(z\,\lambda_2)\,P_-\,\lambda_2}{2\,k_1\,S},
$$

$$
M_{13} = \frac{g\,\sinh(z\,\lambda_1)\,P_+\,\lambda_1}{2\,k_1\,S} - \frac{g\,\sin(z\,\lambda_2)\,Q_-\,\lambda_2}{2\,k_1\,S},
$$

$$
M_{14} = -\frac{d\,g\,\cos(z\,\lambda_2)}{S} + \frac{d\,g\,\cosh(z\,\lambda_1)}{S},
$$

$$
M_{21} = \frac{d^2\,g^4\,\sinh(z\,\lambda_1)\,Q_-}{P\,S\,\lambda_1} - \frac{d^2\,g^4\,\sin(z\,\lambda_2)\,P_+}{Q\,S\,\lambda_2},
$$

$$M_{24} = \frac{d\,g\,\sinh(z\,\lambda_1)\,Q_-}{2\,S\,\lambda_1} + \frac{d\,g\,\sin(z\,\lambda_2)\,P_+}{2\,S\,\lambda_2},$$

$$M_{33} = \frac{Q\,\cos(z\,\lambda_2)}{2\,S} + \frac{P\,\cosh(z\,\lambda_1)}{2\,S},$$

$$M_{34} = \frac{d\,\sinh(z\,\lambda_1)\,P_-}{2\,S\,\lambda_1} + \frac{d\,\sin(z\,\lambda_2)\,Q_+}{2\,S\,\lambda_2},$$

$$M_{43} = \frac{d\,g^4\,\sinh(z\,\lambda_1)\,P_+\,\lambda_1}{k_1\,Q\,S} + \frac{d\,g^4\,\sin(z\,\lambda_2)\,Q_-\,\lambda_2}{k_1\,P\,S}.$$

The remaining entries read: $M_{22} = M_{11}$, $M_{23} = -g^2 M_{14}$, $M_{31} = -M_{24}$, $M_{32} = -M_{14}$, $M_{41} = g^2 M_{14}$, $M_{42} = -M_{13}$, $M_{44} = M_{33}$. Similarly, for the components of the vector r we find

$$r_1 = \frac{k_0}{k_1}\left(\frac{\cosh(z\,\lambda_1)\,Q_+}{2\,S} + \frac{\cos(z\,\lambda_2)\,\hat{Q}_-}{2\,S} - 1\right),$$

$$r_2 = k_0\left(\frac{-Q\,\sinh(z\,\lambda_1)}{2\,S\,\lambda_1} - \frac{P\,\sin(z\,\lambda_2)}{2\,S\,\lambda_2}\right),$$

$$r_3 = k_0\left(\frac{d\,g\,\sinh(z\,\lambda_1)}{S\,\lambda_1} - \frac{d\,g\,\sin(z\,\lambda_2)}{S\,\lambda_2}\right),$$

$$r_4 = \frac{k_0}{k_1}g\left(\frac{\cos(z\,\lambda_2)\,Q_-}{2\,S} + \frac{\cosh(z\,\lambda_1)\,\hat{Q}_+}{2\,S} - 1\right).$$

where $\hat{Q}_+ = Q_+ + 2\,k_1$, $\hat{Q}_- = Q_- + 2\,k_1$.

Having determined the motion in the transverse variables the advancement in the scaled time of flight $\tau = ct$ is found by the equation

$$\tau = \tau_0 + \frac{z}{\beta_0} + \frac{zP_\tau}{\beta_0^2\gamma_0^2}$$
$$+ \int_0^z \frac{1}{2\beta_0}\left[\left(p_x + \frac{k_s}{2}y\right)^2 + \left(p_y - \frac{k_s}{2}x\right)^2\right]dz'.$$

In linear approximation, τ can then be written as

$$\tau = \tau_0 + M_{50} + M_{51}x_0 + M_{52}p_{x0} + M_{53}y_0 + M_{54}p_{y0} + \frac{zP_\tau}{\beta_0^2\gamma_0^2}.$$

While still manageable, the expressions for M_{5*} are somewhat lengthy and will be reported elsewhere [3].

If desired, from the above expressions one can also derive the transfer map in the variables describing deviations from a reference orbit. Consider the transverse motion first. Let ζ_r denote the (on-momentum) reference orbit with initial conditions ζ_{0r}. We write a generic and reference orbit as $\zeta(z) = M(z, P_\tau)\zeta_0 + r(z, P_\tau)$ and $\zeta_r(z) = M(z, 0)\zeta_{r0} + r(z, 0)$, having emphasized the dependence of the quantities M and r on the relative energy deviation P_τ. We subtract the two equations and find for the transverse deviation variables Z

$$Z \equiv \zeta - \zeta_r \simeq M(z,0)Z_0 + \left(\frac{\partial M(z,P_\tau)}{\partial P_\tau}\bigg|_{P_\tau=0}\zeta_{r0}\right.$$
$$\left. + \frac{\partial r(z,P_\tau)}{\partial P_\tau}\bigg|_{P_\tau=0}\right)P_\tau \qquad (1)$$

Table 1: PEP-II Tunes as Computed with MAD and AT.

	Horizontal Tune		Vertical Tune	
	MAD	AT	MAD	AT
HER	24.5225	24.5284	23.6107	23.6190
LER	38.5055	38.5240	36.6360	36.6216

through first order in P_τ, where $Z_0 = \zeta_0 - \zeta_{r0}$. The term in parenthesis corresponds to the R_{*6} entries of the 6×6 transfer matrix R.

As for the time of flight with respect to the reference particle we have

$$T \equiv \tau(z) - \tau_r(z) \simeq M_{51}X_0 + M_{52}P_{X0} + M_{53}Y_0$$
$$+ M_{54}P_{Y0} + \left(\frac{\partial M_{50}}{\partial P_\tau} + \frac{z}{\beta_0^2\gamma_0^2}\right)P_\tau, \qquad (2)$$

valid through first order in P_τ.

APPLICATION TO PEP-II

We have implemented the symplectic integrator for a combined solenoid-dipole-quadrupole field in the Accelerator Toolbox (AT) developed by A. Terebilo [2].

We applied the integrator to the modelling of the IP region of PEP-II [4] for both the High (HER) and Low (LER) energy rings. In the IP region the 1.5 T field from a 4 m long solenoid is superposed on those of dipoles and quadrupole magnets required to separate and focus the colliding beams.

The lattice model for the region as implemented in the MAD decks currently in use consists of a sequence of a large number of interleaved slices of solenoid and combined-function quadrupole/dipole magnets. Besides the sheer size that makes it cumbersome to manage, a drawback of the model is that it is not self-contained. Its implementation requires a prior evaluation of the reference orbit with the solenoid switched off. This information is then used to account for the effect of the solenoid on the vertical closed orbit, by insertion of suitable vertical kicks (MAD assumes that solenoids are centered on the reference orbit).

Models for the interaction regions in each of the PEP-II rings (LER and HER) were constructed as follows.

The region spanned by the solenoid field was divided into 20 sections, with each of the quadrupole magnets QD1 [4] contained therein divided into three sections, and each dipole B1 divided into two sections. Each of the solenoid regions between the quadrupole and dipole magnets was divided into two. At each end of the solenoid, this gives a rather crude model for the roll-off of the solenoid field along the beam trajectory. First approximations for the strengths of the different field components in each section were found by taking the integrated field strength of the section from the MAD model.

The parameters of the components representing the different sections were adjusted to give better agreement with the dynamics in the MAD model. The solenoid and
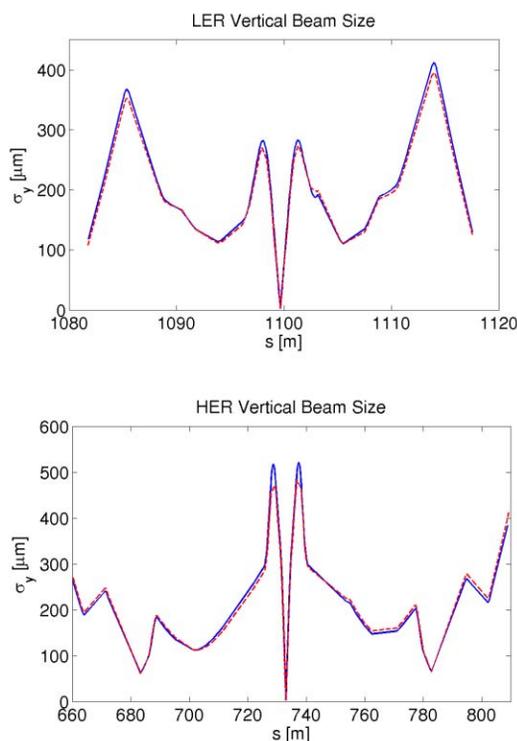
Figure 1: LER (top picture) and HER (bottom picture) vertical beam size as computed with MAD (blue line) and AT (red line).

Figure 2: LER: (top picture) and HER (bottom picture) vertical dispersion as computed with MAD (blue line) and AT (red line).

quadrupole strengths were adjusted to minimize the deviation of the transverse terms of the transfer matrix, first from the entrance of the solenoid to the IP, then from the entrance of the solenoid to the exit of the solenoid. The dipole strengths were adjusted to match the orbit in MAD. For both the LER and HER, adjustments of no more than a few percent were needed from the "nominal" integrated values to give optimum fits to the orbit and the transfer matrices.

No attempt was made to fit the energy or time of flight components of the transfer matrices: these were allowed to take the values arrived at by fitting only the orbit and the components of the transfer matrices relating just to the transverse co-ordinates.

The models of the interaction regions based on the "combined" elements were then used in full lattice models in AT, with the definition of components outside the interaction region taken from the MAD decks. This allows an analysis of the closed orbit, dispersion, beam sizes and tunes for the models using combined elements in the interaction region.

The lattice tunes are shown in Table 1. The transfer matrices across the solenoid (not reported here) calculated using the two methods are within a fraction of percent for the transverse degrees of freedom and few percent for the entries relative to the time of flight. Selected plots of dispersions, and beam sizes are shown in figures 1-2. The beam sizes are calculated using the nominal horizontal emittance, a vertical emittance that is 1% of the horizontal, and the
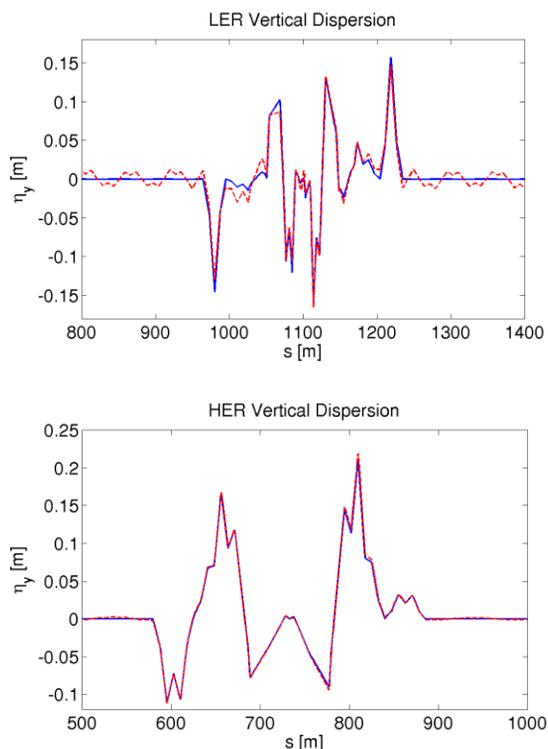
nominal energy spread. There is good agreement for the transfer matrices, orbits and horizontal dispersion between the detailed MAD model using the sliced solenoid, and the AT model using combined elements. In the LER, there is some residual vertical dispersion; there is also some discrepancy in the beam tilts between the two models. There are indications that the poor fits in the LER vertical dispersion and in the HER and LER beam tilts are the result of an inaccurate modelling of the solenoid field, particularly at the ends of the solenoid. We have found it possible, by trial and error, to improve the match in specific parameters by adjusting the strengths of the solenoid components at the ends of the solenoid. In particular, we feel that modelling the roll-off of the solenoid field in just two "steps" is insufficient to achieve a good agreement between the AT and the MAD models. In future works we plan to investigate the possible use of orbit response matrix data for calibrating the IP magnet parameters.

REFERENCES

[1] H. Grote and F. C. Iselin, The MAD Program, CERN Report CERN/SL90-13.

[2] A. Terebilo, http://www-ssrl.slac.stanford.edu/at.

[3] A. Wolski and M. Venturini, LBNL Report, to appear.

[4] Y. Nosochkov et al., SLAC-PUB-7752, 1998.